Internal Stability of Reinforced Soil Retaining Structures with Cohesive Backfills

Y. H. WANG AND M. C. WANG

Reinforced soil retaining structures typically are constructed with cohesionless backfills. It is not uncommon, however, that for economic reasons or because the desired cohesionless backfills are unavailable, locally available cohesive soils are used to construct retaining structures. Little information on the performance of reinforced cohesive soil retaining structures is available. Thus, the performance data of some field and model tests and the results of analysis concerning the internal stability of the structures reinforced with polypropylene strips are presented. The in situ testing was conducted for three retaining structures in China, and the model tests were performed in the laboratory of the Changsha Railway Institute. Data analyzed include lateral earth pressure, vertical pressure, tensile strip force, rupture surface, and lateral facing deformation. The results of analysis show that the lateral earth pressure along the back side of the facing decreases with depth from at-rest pressure at the top to less-than-active pressure at depth. The vertical pressure distribution along the base of backfill is not uniform; the shape of distribution appears to vary with the stiffness of the soil-reinforcing system. Along reinforcing strips, the strip tensile force exhibits a peak formation, and the peak location is closer to the facing at the bottom than at the top of the backfill. The potential sliding surface cuts the top of the backfill at a distance of about 28 percent of the facing height in cohesive backfills rather than 30 percent, which is generally taken for cohesionless backfills. The available data reveal that structures built with more plastic cohesive backfills may exhibit greater time-dependent performance. It is concluded that reinforced soil retaining structures can be constructed satisfactorily using low to slightly medium plastic cohesive backfills if an adequate drainage system is provided. However, more field data are needed to investigate the long-term stability of reinforced soil retaining structures constructed with more plastic cohesive backfills.

In reinforced soil, the primary function of reinforcing strips is to provide the soil with tensile strength. The magnitude of tensile strength that can be mobilized inside the structure depends on the reinforcing material and bonding between the reinforcing strip and the surrounding soil, among other characteristics. For a given reinforcing material, the greater the bond, the higher the tensile strength. The bond strength increases with increasing friction between the reinforcing strip and the soil. Thus, the backfill material must have high frictional resistance and also must be free draining so that little excess pore water pressure will develop during construction, causing a decrease in strip-soil interface bond. In addition, the backfill material must be noncorrosive with low compressibility and exhibit little time-dependent behavior. For these reasons, cohesionless soils are commonly used as backfill materials for construction of reinforced soil retaining structures. Meanwhile, geotechnical criteria including gradation, soundness, and plasticity characteristics have been specified (e.g., the FHWA specification for metallic reinforcement) (*1–4*). The FHWA specifications have also been recommended for geosynthetics reinforcement (*5*).

Depending on the project location and environmental condition, it is not uncommon that, for economical reasons, local soils are used as the backfill material (*5,6*). The local soils may be cohesive, less permeable, and more compressible than the ideal cohesionless material. These undesirable material properties may harm the stability of the reinforced earth retaining structure.

Two key elements to be considered in the design of reinforced soil retaining structures are the internal stability and the external stability of the structure. For external stability, the structure should be analyzed for safety against sliding, overturning, excessive settlement, bearing capacity failure, and rotational slide through the supporting foundation. Internal stability is concerned with failure within the structure involving breakage or slippage of reinforcing strips, excessive lateral displacement of the facing elements, among others. Currently, very little data are available concerning the internal stability of cohesive soils reinforced with polypropylene strips. To investigate possible adverse effects of undesirable soils on the internal stability, analyses are made for lateral earth pressure, forces in reinforcing strips, lateral displacement of the facing element, and internal failure surface of several polypropylene strip–reinforced soil retaining structures constructed with different types of backfill material. This paper presents the results of the analyses and discusses the effect of soil type on internal stability as well as the engineering significance of the research findings.

INSTRUMENTED REINFORCED SOIL STRUCTURES

Three reinforced soil structures were instrumented to monitor their performance, and a large-scale model test was conducted in the laboratory to investigate the behavior of the model reinforced earth retaining structure under various loading conditions. The field structures and laboratory experiment are described in the following.

Department of Civil and Environmental Engineering, Pennsylvania State University, University Park, Pa. 16802.

Hengyang Retaining Structure

The Hengyang retaining structure is located at both sides of the east approach to the Hengyang-Xiangjiang Highway Bridge in Hunan Province, China. Along the curved approach, the structure on the exterior side (exterior wall) is about 260 m long, and the interior wall is approximately 190 m. The wall height varies from 3.12 to 6.83 m, and the height of instrumented section is 4.5 m. The reinforcing strips are polypropylene strips, each 15 mm wide, 1 mm thick, and 5 m long. Their tensile strength, tensile modulus, and rupture strain are 2.34 kN/strip, 2000 MPa, and 8.0 percent, respectively. The vertical spacing is 50 cm, and the center-to-center horizontal spacing varies between 4 and 7 cm. The backfill material is a silty clay with a liquid limit (LL) of 22.1 percent, plasticity index (PI) of 5.8, internal friction angle (ϕ) of 31.4 degrees, and cohesion (c) of 22.0 kPa. Under the standard Proctor compaction, the maximum dry unit weight (γ_{dmax}) and optimum water content (W_{opt}) are 17.3 kN/m^3 and 19.4 percent, respectively. Each reinforcing strip is surrounded by a thin layer (about 5 cm thick) of a sandy soil; this technique was also used by Sridharan et al. (*7*). The facing was made of plain concrete blocks, each 60 cm long, 40 cm high, and 5 cm thick. The soil was compacted to 95 percent of the maximum based on the standard Proctor compactive effort. The construction started in October 1988 and was completed in June 1989. Field measurements included lateral earth pressure distribution along the back of the facing elements, lateral earth pressure distribution along the back side of the reinforced zone, and tensile force distribution along the reinforcing strip. Details on construction and testing program for the project are available elsewhere (*8*).

Pingshi Retaining Structure

The Pingshi retaining structure supports the platform and building of the Pingshi railroad station in northern Guangdong Province, China. The structure is 50 m long and was originally 7.25 m high, but it was increased to 10 m high 2 years after construction. The reinforcement is provided by polypropylene strips. Each strip is 22.0 mm wide and 1.4 mm thick, having a tensile strength, tensile modulus, and rupture strain of 6.48 kN, 1,910 MPa, and 11.0 percent, respectively. The vertical spacing is 50 cm, and the horizontal center-to-center spacing varies from 5 to 8 cm. There are three strip lengths: 10, 8, and 6 m in the upper, middle, and lower levels, respectively. The details can be found in a research report by Hua et al. (*9*).

The backfill material is a miscellaneous fill, which is a mixture of local cohesive soil with construction debris, with LL = 28.8 percent, PI = 10.1, ϕ = 32.8 degrees, c = 6.5 kPa, γ_{dmax} = 18.7 kN/m^3, and W_{opt} = 15.5 percent. The soil was compacted to 85 percent standard Proctor compaction. The construction began in June 1990 and was completed in October 1990. Field measurements include lateral earth pressure distribution along the back of the facing elements, vertical pressure distribution along the reinforcement layers, tensile force in the reinforcement, vertical and lateral displacements of the facing, and others.

Yueyang Retaining Structure

The third retaining structure is at the Yueyang Municipal Weather Observatory Station. It is 75 m long and 18 m high (maximum) and reinforced with polypropylene strips. Each strip is 14.5 mm wide and 0.87 mm thick; tensile strength, tensile modulus, and rupture strain are 1.85 kN, 1650 MPa, and 10.0 percent, respectively. According to Wang et al. (*10*), the length of reinforcing strips equals 20 m in the upper 4 m of the facing, 12 m in the next 4 m, 9 m in the following 4 m, and 7 m in the bottom 6 m of the facing. The backfill material is a cohesive soil with LL = 34.5 percent, PI = 9.2, ϕ = 28.5 degrees, c = 31.0 kPa, γ_{dmax} = 17.4 kN/m^3, and W_{opt} = 18.5 percent. Field measurements include reinforcing strip force and lateral and vertical displacements of the facing elements.

Laboratory Model Test

The laboratory model reinforced soil retaining structures are constructed on a concrete floor; each is 2.0 m high, 1.8 m wide, and 3.1 m long. The reinforcing strips are made of polypropylene. Seven tests were performed: a fine sand was used as the backfill material in five tests, and a silty clay was used in two tests. The fine sand backfill has ϕ = 35.0 degrees, γ_{dmax} = 17.2 kN/m^3, and W_{opt} = 9.5 percent; the silty clay backfill has LL = 30.6 percent, PI = 10.4, ϕ = 26.1 degrees, c = 16.0 kPa, γ_{dmax} = 17.9 kN/m^3, and W_{opt} = 16.5 percent. Measurements taken were tensile force in the reinforcing strips, vertical pressure distribution along the reinforcement, lateral pressure distribution along the facing, lateral deformation of the facing, and others. Detailed descriptions of the test model and measurement program are documented by Wang et al. (*11*).

LATERAL EARTH PRESSURE

The lateral earth pressure along the back side of the facing obtained from the Hengyang and Pingshi test sites and laboratory model testing are shown in Figure 1. Note that no lateral pressure data are available from the Yueyang project and that the data obtained from the Yoajian project by Wang et al. (*12*) and from the Yinshanzhen project by Wu (*13*) are also included in the figure for comparison.

As would be expected, the data points in Figure 1 are scattered because of testing errors, instrumentation problems, and possibly other mistakes. For instance, the negative lateral pressure shown in the Hengyang project is probably a result of malfunction of the pressure gauge. Also, the much greater fluctuation of the data points at the bottom of the facing in the Yinshanzhen project (*13*) probably resulted from a less-than-perfect gauge performance. Despite these irregularities, a trend is clear that except for two cases, the lateral pressure increases with depth at a decreasing rate. One case is the laboratory model test, with a cohesive backfill for which the lateral pressure is almost zero throughout the entire facing. The other case is the Yaojian project (*12*), in which the lateral

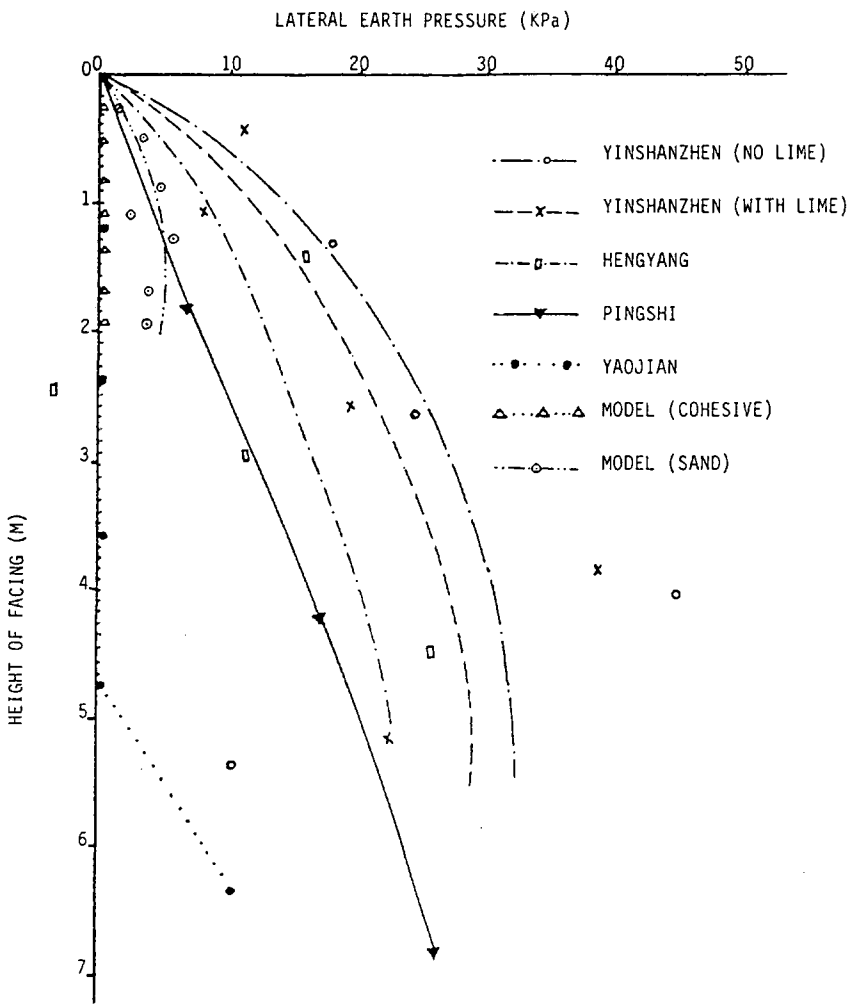

FIGURE 1 Lateral earth pressure data from different projects.

pressure is very small to the depth of about 4.8 m and then increases with depth.

Comparing the two curves of laboratory model tests, it is seen that the lateral pressure of the cohesive backfill is much smaller than that of the cohesionless backfill and is nearly equal to zero over the entire facing. One possible explanation for the near-zero pressure is that the backfill is in a state of tension. According to the Rankine theory, the cohesive backfill with c = 16 kPa, ϕ = 26.1 degrees, and γ = 17 kN/m^3 has a critical height of about 3.0 m, which exceeds the height of the facing. It should be noted, however, that this reasoning ignores the effect of reinforcement: with reinforcement, the shear strength behavior is different, so the depth of tension zone must be different.

Another important point is the effect of the construction process on lateral earth pressure. In construction, the backfill is normally deposited in layers and compacted longitudinally (parallel with the facing) starting from the mid-section and moving gradually toward the end and then back to the facing. Near the facing, compaction was done carefully with a hand-operated vibratory compactor. When the backfill is densified, the soil behind the facing displaces laterally, inducing a lateral earth pressure on the facing. Such a construction-induced lateral earth pressure can be minimized relatively more easily in the laboratory model test, but not in the field test. Of the five field projects shown, it appears that the construction-induced lateral pressure was greatly minimized in the Yaojian project. However, considerable lateral earth pressures are seen in the data of the Pingshi, Hengyang, and Yinshanzhen projects.

It should be noted, however, when the various sets of test data are compared directly, that in addition to the types of backfill and reinforcing strip, construction parameters also influence the lateral earth pressure distribution. Some important construction parameters are the method of placing reinforcing strips and backfills, compaction method, speed of construction, and facing elements. The effect of these factors on the performance of reinforced retaining structures has been discussed by Jones (*14*).

For design purposes, the construction-induced lateral earth pressure must be taken into consideration. Thus, each of these data sets is smoothed by a curve. On the basis of this curve, the ratio K/K_a is computed and plotted against depth in Figure 2. The figure shows that, except for the Yaojiang project, the range of K/K_a values at the same depth for the various backfill soils falls within a relatively narrow range. A trend is clearly

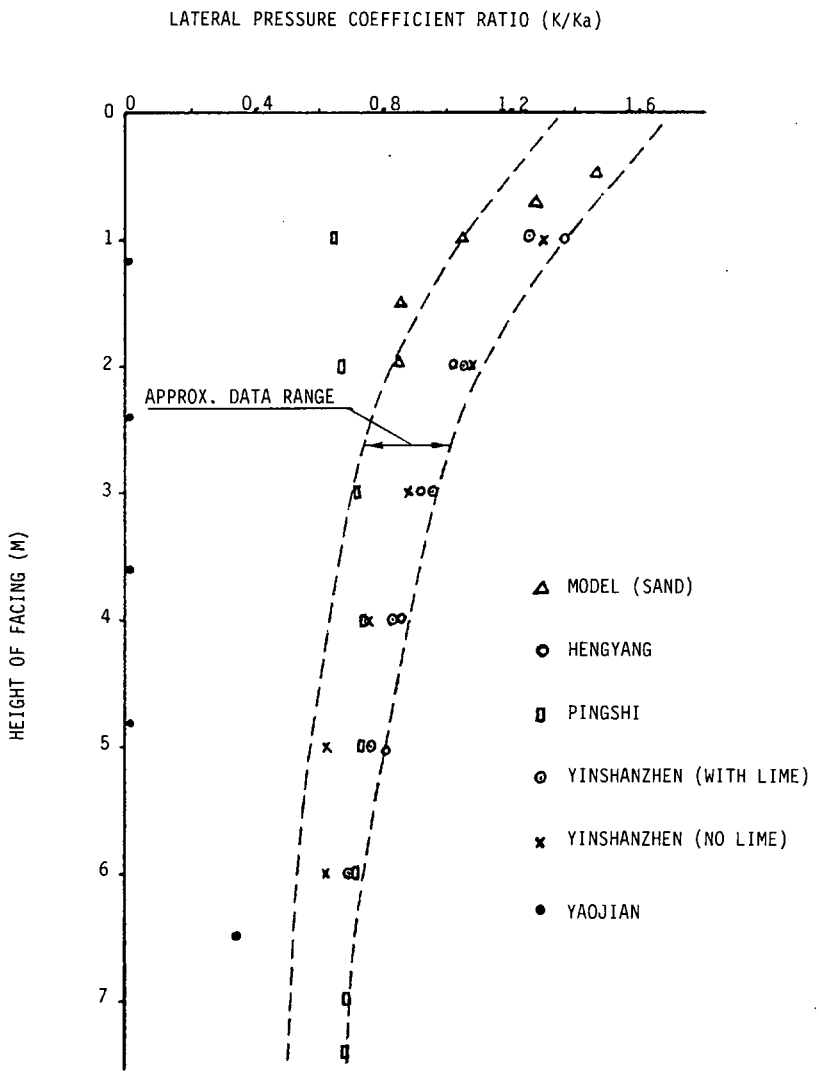

FIGURE 2 Distribution of lateral pressure coefficient ratio with facing height.

shown that the lateral earth pressure coefficient, K, at the backfill surface is greater than K_a and decreases with increasing depth to less than K_a.

Of the five projects reported, the lateral earth pressure measurements were taken at different times in two projects: Yinshanzhen and Hengyang. The results of the Yinshanzhen project (*13*) of which the data were obtained during construction, at 6 months, and at 1 year after, showed that the lateral earth pressure increased from slightly greater than K_a to about K_o in the first 6 months and became almost constant thereafter. However, no appreciable change in lateral pressure was observed in the Hengyang project (*8*) during 3 years after construction. Note that the cohesive backfills have an LL of 22.1 percent and a PI of 5.8 for Hengyang and an LL of 31.8 percent and a PI of 11.3 for Yinshanzhen. Since the Yinshanzhen backfill is slightly more plastic than the Hengyang backfill, the data reveal that cohesive backfills with higher plasticity may undergo more significant increases in lateral earth pressure with time at least for about a year after construction. More field data are needed, however, to establish the relationship between time-dependent lateral pressure and plasticity characteristics.

VERTICAL PRESSURE

The vertical pressures acting on the base of the retaining structures are shown in Figure 3. The figure contains the data of laboratory model tests and field tests from the Pingshi, Xiaolongtan, and Jiangcun projects (*15,16*). No pressure distribution data from the Hengyang, Yinshanzhen, and Yaojian projects are available. Also included in the figure for comparison is the vertical geostatic stress, which is equal to the product of soil unit weight and depth for each condition. The model test data for both cohesive and cohesionless backfills are very close to each other. It appears that the vertical pressure increases linearly from the facing to the back of the structure and that the average pressure is approximately equal to the computed geostatic stress.

Other data sets are more scattered, and the shape of the pressure distribution for each case is more erratic. However, some cases (e.g., the Xiaolongtan and Pingshi projects) reveal a trend of bilinear distribution of which the vertical pressure first increases and then decreases with distance from the facing. The data from the Jiancun structure appear to reveal a linear distribution similar to that of the model test data but

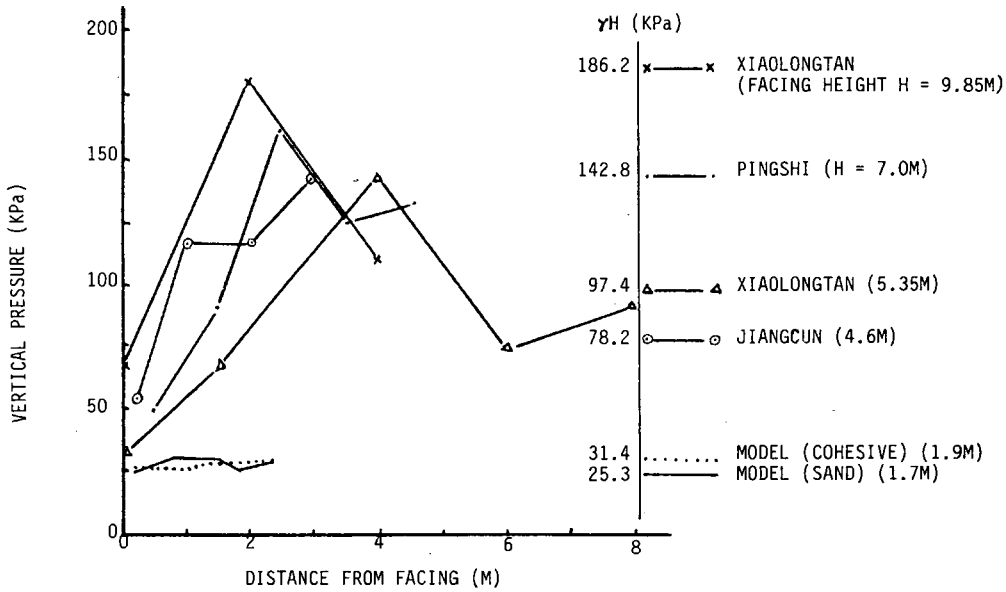

FIGURE 3 Vertical pressure distribution along base of backfill and computed geostatic vertical pressure.

with a much greater rate of pressure variation. There appears to be no distinct difference in vertical pressure distribution between the cohesive and cohesionless fills. One thing that is quite clear, however, is that the vertical pressure at the facing is the smallest along the base of the structure. Furthermore, the measured vertical pressure except for the model test is very different from the vertical geostatic stress.

The vertical pressure distribution along the base of a reinforced soil retaining structure may vary with many factors. The more important influencing factors are the uniformity and stiffness of the structure proper, the uniformity and rigidity of the supporting foundation, and the type and condition of the material behind the structure (backfill material). For a more uniform and stiffer structure, a less erratic vertical pressure distribution can be expected. With a compressible supporting foundation, the weight-induced settlement increases gradually from the facing to the back of the structure, resulting in a different vertical pressure distribution than that with a rigid foundation base.

To satisfy the requirement of elastic equilibrium, a smaller vertical pressure under the facing can be expected if the entire system including the structure, backfill material, and supporting foundation are treated as elastic media. On the other hand, the weight-induced sagging settlement may cause the structure to tilt against the backfill soil, inducing additional lateral earth pressure. The lateral earth pressure including the originally existing and the additional value may alter the vertical pressure distribution along the base. The degree of alteration depends on not only the magnitude of lateral earth pressure but also the stiffness of the retaining structure. Generally speaking, under a given lateral earth pressure, greater alteration in vertical pressure distribution along the base of the structure may take place as the structure stiffness increases.

On the basis of the preceding information, a less erratic vertical pressure distribution in the test model than the distributions in the field tests can be expected, because material nonuniformity can be minimized through a better controlled construction of the test model. Meanwhile, a rigid concrete floor can provide a more uniform firm foundation support for the structure. Another factor that should be considered in comparisons is that no lateral earth pressure exists on the back side of the test model. As a result, a uniform vertical pressure distribution is seen for the test model.

In the Yinshanzhen project, the vertical pressure was measured at a few selected places for three times: on completion of construction, 6 months after, and 1 year after. The data showed that the vertical pressure in the top 3 m of the backfill increased substantially with time, whereas below 3 m the vertical pressure did not change significantly with time. No sufficient data indicate a definite trend of increasing vertical pressure with time.

TENSILE FORCE IN REINFORCEMENT

The tensile forces measured from two sets of reinforcing strips in model tests are shown in Figure 4 (*left*) for cohesionless backfill and Figure 4 (*right*) for cohesive backfill. For convenience, the two strips are labeled Strips A and B. Generally speaking, despite some discrepancy, the two curves A and B match each other fairly well. The data for cohesionless backfill show more clearly that the location of peak tensile force is closer to the facing at bottom than at top. Meanwhile, the data appears to reveal that the peak tensile force reaches a maximum at about mid-height of the facing in cohesionless backfill. A comparison between the cohesive and cohesionless backfills indicates that, in the cohesive backfill, the strip tensile force is considerably smaller and the peak force does not vary substantially with depth. The curves are much flatter in cohesive than in cohesionless backfills.

Some of the tensile force data obtained from field tests are shown with those of model tests in Figure 5. To consider the effect of overburden pressure, the tensile force is expressed as a dimensionless ratio of $T/\gamma H^3$, in which T, γ, and H are

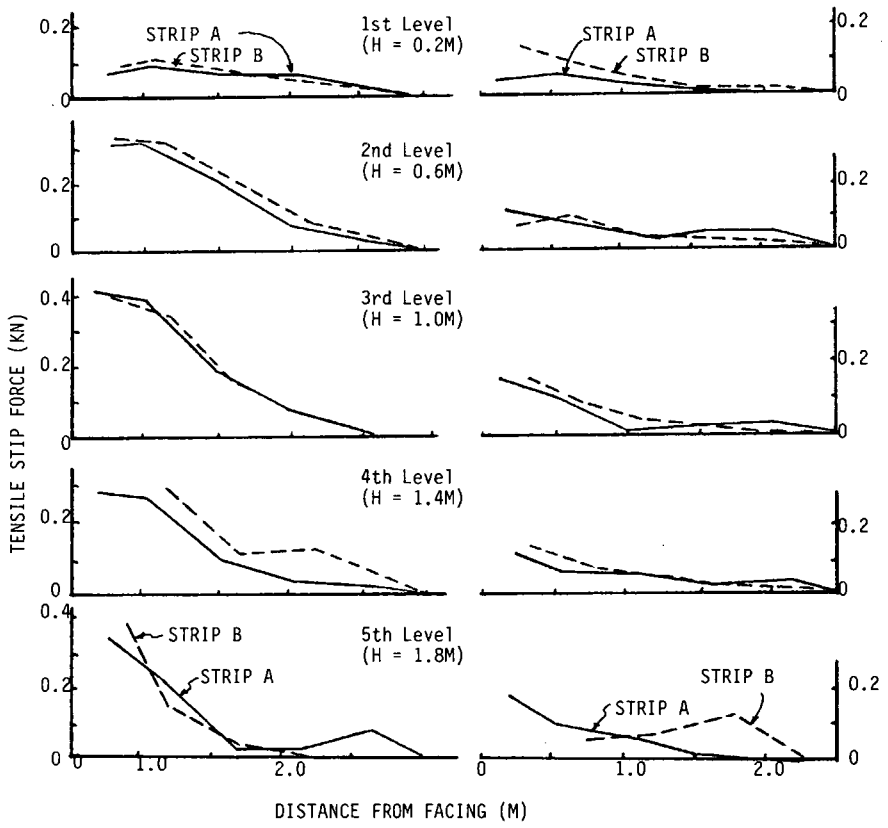

FIGURE 4 Tensile strip force distribution in model tests: *left*, sand backfill; *right*, cohesive backfill.

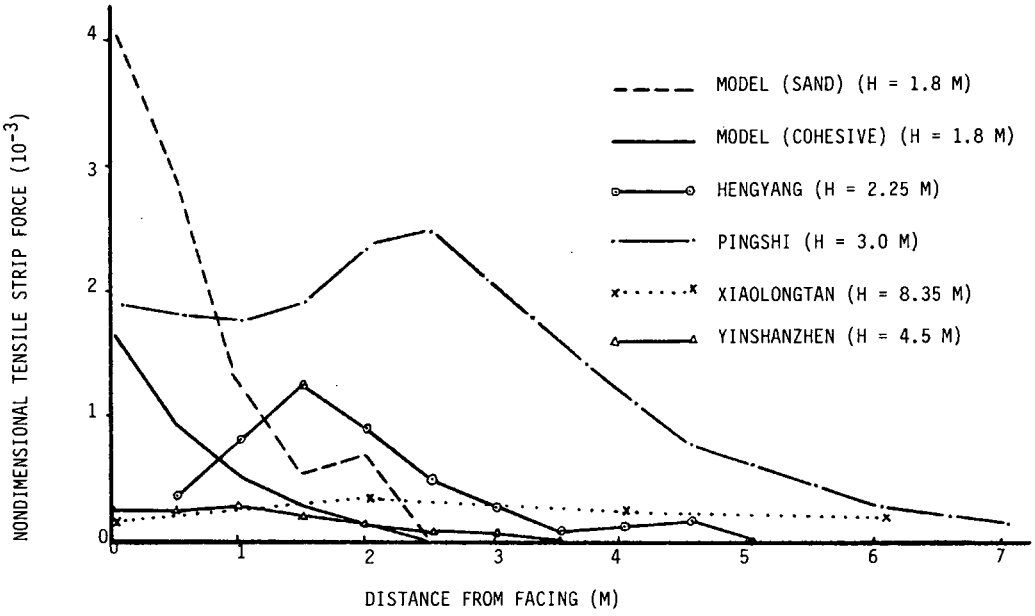

FIGURE 5 Nondimensional tensile strip force ($T/\gamma H^3$) distribution along strip.

tensile force, soil unit weight (in kilonewtons per cubic meter), and overburden height, respectively. The overall trend reveals that the value of $T/\gamma H^3$ does not vary considerably with cohesion but appears to increase with increasing internal friction angle. However, a direct numerical comparison among the various curves is difficult because of the influence of many factors, including the relative position of the reinforcing strip in terms of the total height of facing, construction process, and lateral displacement of the facing.

As for the effect of time, the data of the Yinshanzhen project reveal that within a year after construction, the tensile strip force increased by about 50 percent and the position of peak tensile force moved slightly toward the facing (*13*). But no appreciable changes in the magnitude of tensile force and the location of peak force were observed during 3 years after construction in the Hengyang project. As mentioned in the discussion of lateral earth pressure, the Yinshanzhen backfill is more plastic than the Hengyang backfill. Thus, it appears that the more plastic the cohesive backfill is, the more pronounced the time-dependent tensile strip force may be.

LATERAL DEFORMATION OF FACING

The lateral deformation data of the model tests, one with a cohesionless backfill and the other with a cohesive backfill, are shown in Figure 6. As shown, the maximum lateral deformation does not take place at top of the backfill. Furthermore, the maximum lateral deformation for cohesionless backfill is as high as seven times greater than that for cohesive backfill. The shape of the deformation profile is also quite different in that at bottom, significant deformation takes place and the curvature of the profile is sharper for cohesionless than cohesive backfills.

Besides the type of backfill material, many other factors affect lateral facing deformation. More important factors include facing height, stiffness of facing elements, design and stiffness of reinforcing system, compaction process, construction method, and elapsed time. Therefore, it is difficult, if not impossible, to quantify the lateral facing deformation from these influencing factors.

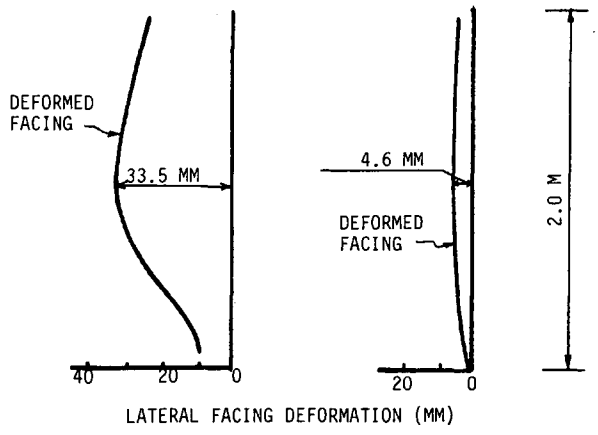

FIGURE 6 Lateral facing deformation in model tests: *left*, sand backfill; *right*, cohesive backfill.

The field data of the Yinshanzhen project demonstrated that the maximum lateral facing deformations on completion of construction were approximately 1.2 percent of the total facing height for the cohesive backfill. The lateral deformation increased by about 5 percent at 6 months after construction and remained almost constant thereafter. In the Pingshi project (*9*), the maximum lateral facing deformation increased by about 7 percent 2 years after construction. However, the field data of other projects did not show appreciable increase in facing deformation with time after the completion of construction. These projects include Hengyang, which was completed in August 1988 (*8*); Duizhen, constructed in 1984 (*17*); and Kouzhen, completed in October 1984 with an initial maximum facing deformation equal to approximately 1 percent of the facing height (*17*).

The backfill materials of these projects varied considerably. As mentioned earlier, the LLs and PIs are 31.8 percent and 11.3, respectively, for the Yinshanzhen backfill; 28.8 percent and 10.1 for the Pingshi backfill; and 22.1 percent and 5.8 for the Hengyang backfill. Both Duizhen and Kouzhen backfills are loess, having γ = 17.8 kN/m^3, ϕ = 42 degrees, and c = 8 kPa for Duizhen, and γ = 18.5 kN/m^3, ϕ = 45 degrees, and c = 9 kPa for Kouzhen. Their LL and PI estimated from related data (*17*) are 29 percent and 10, respectively. According to the plasticity chart, these backfill soils are low to slightly medium plastic. Loess and cohesive soils with low PIs do not appear to undergo significant increase in facing deformation. For backfills with higher PIs, the lateral facing deformation will increase slightly with time in the first or second year after construction. More data are needed to draw a more definite conclusion, however.

POTENTIAL RUPTURE SURFACE

In common practice, the potential failure surface is taken at the surface that connects the point of peak tensile force in each reinforcing strip. As mentioned earlier, for cohesionless backfills, an often-used approximation is that the potential failure surface is bilinear, consisting of a vertical plane in the upper half and an inclined plane in the lower half of the facing. The horizontal distance from the facing along the top of backfill equals 0.3 H (H is facing height in meters), and the oblique plane makes an angle of 45 degrees + ϕ/2 from the horizontal (*2–4*). For cohesive backfills, the horizontal distance on top of the backfill between failure surface and facing is estimated from the location of peak tensile force in the uppermost row of reinforcing strips. Results of the field tests and other available data, including those of the Duizhen project, are given in Table 1. It is seen that the horizontal distance varies between 0.24 and 0.32 H. From these data, it is reasonable to take 0.28 H as the horizontal distance between facing and failure surface for cohesive backfills.

EARTH PRESSURE COEFFICIENTS

The internal stability analysis of reinforced earth retaining structures requires a method for determining lateral earth pressure. From the data presented in Figure 2 and design experience, the lateral pressure coefficient diagram shown in

TABLE 1 Position of Failure Surface

Projects	Height of Facing, H (m)	Backfill Materials					Horizontal Distance on Top of Backfill from the Facing to Failure Surface, (m)	References
		Type of Backfill	Degree of[a] Compaction, (%)	Plasticity Index, (%)	Internal Frictional Angle, ϕ (deg.)	Cohesion, c (kpa)		
Yinshanzhen	5.66	cohesive soil with 2% of lime	91	11.3	28.0	6.2	0.24H	(13)
Hengyang	5.37	silty clay	92	5.8	31.4	22.0	0.28H	(8)
Duizhen	4.72	loess	91	10.4	42.0	8.0	0.28H	(17)
Pingshi	7.25	miscellaneous fill	85	10.1	32.8	6.5	0.30H	(9)
Yaojian	7.40	loess	90	15.4	37.2	9.0	0.32H	(12)
Xiaolongtan	10.35	crushed stone with sand and clay	93	3.5	29.5	8.0	0.25H-0.30H	(15)

[a] based on Standard Proctor Compactive effort

Figure 7 is proposed for use in analysis and design of reinforced earth retaining structures containing different types of backfills. The mathematical expressions of Figure 7 are as follows:

$$K = K_o - \frac{z}{5}(K_o - K_a) \qquad \text{for } 0 < z \leq 5\text{m} \tag{1}$$

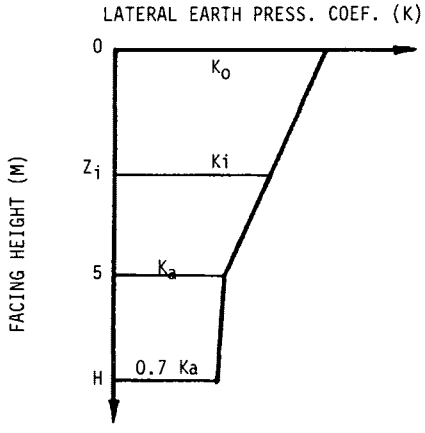

FIGURE 7 Proposed lateral earth pressure coefficient distribution along facing (K_i = value of K at Z_i below top of backfill).

$$K = \left[1 - \frac{0.3(z - 5)}{H - 5}\right]K_a \qquad \text{for } 5 < z \leq 10\text{m} \tag{2}$$

where

K = lateral earth pressure coefficient at z,
z = depth measured from top of backfill (m),
K_o = coefficient of lateral earth pressure at rest
= $\mu/(1 - \mu)$,
μ = Poisson's ratio of backfill material, and
K_a = coefficient of active earth pressure
= $\tan^2$ (45 degrees $- \phi/2$).

To demonstrate the effectiveness of the proposed lateral earth pressure coefficients, a comparison is made in Table 2 between the computed and the measured values of the resultant lateral pressure and its point of application for nine different conditions involving both cohesive and cohesionless backfills. It is seen that the measured data are much smaller than the computed values for the model tests and the Yaojian project, primarily because the computed values have taken into consideration the construction-induced pressures. For these tests, the construction-induced pressure is very small, as mentioned earlier. Therefore, the computed value exceeds the measured value as high as 100 percent for the model test with cohesive backfill, 34.4 percent for the Yaojian project, and 21.1 percent for the model test with cohesionless backfill. Except for these three data sets, a close agreement between the computed and measured data is seen. Further, the great majority of the data show that the computed are greater than

TABLE 2 Comparisons Between Computed and Measured Lateral Earth Pressures

Projects	Height of the Facing, H (m)	Backfill Materials				Lateral Earth Pressures					References
		Unit Weight (kN/m^3)	Internal Friction Angle, ϕ (deg.)	Cohesion, c (kPa)	Type of Backfill	Computed		Measured		Difference	
						Resultant, Rc (kN/m)	Point of Application from Bottom	Resultant, Rm (kN/m)	Point of Application from Bottom	$\frac{R_c - R_m}{R_c}$ (%)	
Pingshi	7.25	18.0	33.0	6.5	miscellaneous fill	104.3	0.38H	97.9	0.35H	6.1	(9)
Hengyang	4.75	18.6	26.1	22.0	silty clay	50.5	0.39H	52.9	0.42H	-4.8	(8)
Xiaolongtan	10.35	18.7	24.4	3.1	crushed stone with sand and clay	336.7	0.38H	321.0	0.36H	4.7	(15)
Jiangcun	4.60	17.0	35.0	0	coarse sand with crushed stone	60.9	0.36H	59.0	0.32H	3.1	(16)
Model test	2.00	17.3	35.0	0	find sand	9.5	0.34H	7.5	0.38H	21.1	(11)
Model test	2.00	17.4	26.1	16.0	silty clay	8.3	0.36H	0	-	100	(11)
Yinshanzhen	5.66	22.6	22.0	5.0	cohesive soil	122.9	0.38H	123.0	0.34H	-0.1	(13)
Yinshanzhen	5.66	22.4	28.0	6.2	cohesive soil with 2% lime	115.0	0.38H	114.1	0.35H	0.8	(13)
Yaojian	7.40	21.9	37.2	9.0	Loess	93.2	0.40H	61.1	0.12H	34.4	(12)

the measured values. Thus, use of the proposed lateral earth pressure coefficients may provide some degree of conservativeness in the designed structures.

REMARKS

The lateral earth pressure on the facing depends not only on backfill properties but also on the construction process. Normal construction induces considerable lateral pressures that should be considered in the analysis and design of reinforced-earth retaining structures. The proposed lateral earth pressure coefficients have considered such a pressure component, and therefore should be able to provide more reliable lateral earth pressures. It should be pointed out that the proposed lateral earth pressure coefficients differ from Schlosser's coefficients (*18*) in that at depths the lateral pressures computed from Schlosser's coefficients are substantially greater than those computed from the proposed coefficients. Experience has shown that the lateral pressure obtained from Schlosser's coefficients often yielded excessive reinforcement, resulting in unreasonably narrow strip spacings at the lower portion of the backfill.

The vertical pressure distribution along the base of the backfill differs from that of the conventional gravity retaining structure. The available data suggest that factors such as backfill type, design and construction of the reinforcing system, and stiffness of the supporting foundation are important in controlling the shape of pressure distribution. More field data are required to determine the relationship between vertical pressure distribution and the influencing factors. The shape of the tensile strip force distribution has no considerable difference between cohesive and cohesionless backfills. However, the magnitude of tensile force is substantially smaller in cohesive than in cohesionless backfills. Further, the location of the potential rupture surface is slightly closer to the facing for cohesive than cohesionless backfills. These suggest that in cohesive backfills, the reinforcing strips can be shorter and also more widely spaced than in cohesionless backfills.

From the available field data, an increase with time in lateral earth pressure, tensile strip force, and lateral facing deformation has been observed in some structures constructed with cohesive backfills. However, no adverse effect has resulted from such a behavior. So far, all retaining structures have performed satisfactorily. It should be pointed out, however, that adequate surface and subsurface drainage systems are needed to maintain the as-constructed backfill property. Since the backfills investigated range from low to slightly medium plastic soils, further study is needed to investigate the long-term stability of reinforced earth retaining structures built with more plastic cohesive backfills.

SUMMARY AND CONCLUSIONS

To investigate the effectiveness of using cohesive backfills for construction of polypropylene strip-reinforced soil retaining structures, laboratory model tests and in situ field tests were performed. Four cohesive soils and one cohesionless soil were studied. Performance measurements included the lateral and vertical pressures, tensile strip force, and lateral deformation of the facing. In addition to the test data, available information was also used in the analysis and evaluation.

Test data show that the lateral earth pressure coefficient along the back side of the facing decreases with depth from a maximum at the top of backfill. At the top, the maximum pressure is approximately equal to the at-rest pressure, and at greater depths the pressure becomes less than the active pressure. The vertical pressure along the base of backfill is not uniformly distributed; however, no conclusive data indicate a definite pattern of pressure distribution. The tensile force in reinforcing strips increases with distance from the facing to a maximum, then decreases. The tensile strip force is smaller in cohesive than in cohesionless backfills. The shape of the potential rupture surface in cohesive backfills is a little closer to the facing than that in cohesionless backfills. The available data reveal that the structure with more-plastic cohesive backfills may exhibit more pronounced time-dependent performance.

From the results of this study, it may be concluded that low to slightly medium plastic cohesive soils can be used to construct satisfactory reinforced soil retaining structures, if adequate surface and subsurface drainage systems are provided. However, more field test data are required to determine possible long-term effects of the time-dependent behavior of more-plastic cohesive backfill on the stability of the retaining structures.

ACKNOWLEDGMENT

The manuscript was painstakingly typed by Karen M. Detwiler, for which the authors are appreciative.

REFERENCES

1. Christopher, B. R., S. A. Gill, J.-P. Giroud, I. Juran, J. K. Mitchell, F. Schlosser, and J. Dunnicliff. *Design and Construction Guidelines for Reinforced Soil Structures*, Vol. 1. Report FHWA-RD-89-043. FHWA, U.S. Department of Transportation, 1989.
2. Mitchell, J. K., and W. C. B. Villet. *NCHRP Report 290: Reinforcement of Earth Slopes and Embankments*. TRB, National Research Council, Washington, D.C., June 1987.
3. Jones, C. J. F. P., *Earth Reinforcement and Soil Structures*. Butterworth, London, England, 1985.
4. Yamanouchi, T., N. Miura, and H. Ochiai. *Theory and Practice of Earth Reinforcement*. Balkema, Rotterdam, The Netherlands, 1988.
5. Zornberg, J. G., and J. K. Mitchell. *Poorly Draining Backfills for Reinforced Soil Structures—A State of the Art Review*. Geotechnical Engineering Report UCB/GT/92-10. Department of Civil Engineering, University of California, Berkeley, Oct. 1992.
6. Temporal, J., A. H. Craig, D. H. Harris, and K. C. Brady. The Use of Locally Available Fills for Reinforced and Anchored Earth. *Proc., 12th International Conference on Soil Mechanics and Foundation Engineering*, Vol. 2, Rio de Janeiro, Brazil, Aug. 1989, pp. 1315–1320.
7. Sridharan, A., B. R. S. Murthy, Bindumadhava, and K. Revanasiddappa. Technique for Using Fine-Grained Soil in Reinforced Earth. *Journal of Geotechnical Engineering*, ASCE, Vol. 117, No. 8, Aug. 1991, pp. 1174–1190.
8. Wang, Y. H. Testing and Research of the Reinforced Earth Wall. *Journal of Changsha Railway Institute* (in Chinese). Vol. 7, No. 4, Dec. 1989, pp. 87–98.
9. Hua, Z. K., Y. H. Wang, and Q. F. Liu. Testing and Studies of the Reinforced Earth Retaining Wall on Heng-Guang Double-Railline. *Proc., 6th Chinese Conference on Soil Mechanics and Foundation Engineering* (in Chinese). Shanghai, June 1991, pp. 487–490.

10. Wang, Y. H., Z. K. Hua, and Q. F. Liu. *The Interpretation of Design Code Clauses for Reinforced Earth Retaining Structures* (in Chinese). Aug. 1991.
11. Wang, Y. H., Z. K. Hua, and Q. F. Liu. *Testing Report of the Laboratory Model for Reinforced Earth Retaining Structures* (in Chinese). 1991.
12. Wang, Z. S., C. C. Li, Y. Yen, and D. L. Yao. Prototype Scale Design and Test of Reinforced Earth Retaining Wall with Cohesive Backfill. *Proc., 3rd National Symposium on Reinforced Earth Engineering* (in Chinese). Oct. 1990, pp. 38–59.
13. Wu, W. L. In-Situ Test and Analysis of the Reinforced Earth Retaining Wall on Cheng-Yu Highway at Yinshanzhen. *Proc., 3rd National Symposium on Reinforced Earth Engineering* (in Chinese), Oct. 1990, pp. 67–108.
14. Jones, C. J. F. P. Construction Influences on the Performance of Reinforced Soil Structures in Performance of Reinforced Soil Structures. *Proc., International Reinforced Soil Conference*, (A. McGown, K. Yeo, and K. Z. Andrawes, eds.), Thomas Telford, London, England, 1991, pp. 98–116.
15. Science Research Department of the 4th Railway Designing Institute (China). The Report of Testing Analysis for Reinforced Earth Retaining Wall at Xiaolongtan of Yunnan Province. *Subgrade Engineering* (in Chinese), Vol. 8, No. 1, 1986, pp. 40–52.
16. Science Research Department of the 4th Railway Designing Institute (China). The Report of Prototype Scale Design, Construction and In-Situ Test for Reinforced Earth Retaining Wall at Jiangcun. *Proc., 3rd National Symposium on Reinforced Earth Engineering* (in Chinese), Oct. 1990, pp. 125–141.
17. J. T. E, Y. L. Xu, and Y. Y. Wu. Report of Prototype Scale Test for Reinforced Earth Retaining Wall at Duizhen. *Proc., 3rd National Symposium on Reinforced Earth Engineering* (in Chinese), Oct. 1990, pp. 62–66.
18. F. Schlosser. History, Current and Future Development of Reinforced Earth. Presented at the Symposium on Soil Reinforcing and Stabilizing Techniques, New South Wales Institute of Technology, Sydney, Australia, Oct. 1978.

Publication of this paper sponsored by Committee on Geosynthetics.